International Journal on Magnetic Particle Imaging
Vol 9, No 1, Suppl 1, Article ID 2303082, 4 Pages

Infinite Science Publishing

Proceedings Article

X-Space Image Reconstruction for Lissajous Trajectory Using Multidimensional Image Tensor

Osmanalp Omeroglu[a,†,*] · Hasan Sabri Melihcan Erol[a,b,†] · Ali Alper Ozaslan[a,c] · Emine Ulku Saritas[a,c,d]

[a] Department of Electrical and Electronics Engineering, Bilkent University, Ankara, Turkey
[b] Department of Electrical Engineering and Computer Science, Massachusetts Institute of Technology, Cambridge, MA, USA
[c] National Magnetic Resonance Research Center (UMRAM), Bilkent University, Ankara, Turkey
[d] Neuroscience Program, Sabuncu Brain Research Center, Bilkent University, Ankara, Turkey
[†] Shared first authorship
[*] Corresponding author, email: osmanalp.omeroglu@ug.bilkent.edu.tr

Abstract

The tensor-based theory of multidimensional x-space MPI provides useful insight into MPI image reconstruction. Using this theory, it was shown that x-space MPI images with isotropic resolution can be achieved by scanning in two orthogonal directions separately and combining the resulting images. In this work, we propose an x-space image reconstruction that resolves the multidimensional image tensor, allowing us to reconstruct the isotropic MPI image for the Lissajous trajectory. The proposed method takes advantage of the self-crossing property of the Lissajous trajectory.

I. Introduction

X-space reconstruction is one of the two leading reconstruction methods in magnetic particle imaging (MPI), together with system function reconstruction [1, 2]. The tensor-based theory of multidimensional x-space MPI allows us to represent the scalar images acquired by receive coils using a single tensor equation at a given field-free point (FFP) position on the scanning trajectory [3]. Using this tensor formalism, it was shown that MPI images with isotropic resolution can be achieved by combining two images acquired with orthogonal choice of 1D drive fields (DFs) [3]. Another work proposed a similar approach followed by deconvolution to achieve high resolution isotropic MPI images [4].

In this work, we propose an x-space image reconstruction technique that resolves the multidimensional image tensor for the Lissajous trajectory, enabling the reconstruction of the isotropic MPI image for this multidimensional DF scenario. We demonstrate two different variants of the proposed method: solving the tensor on the Lissajous node points or solving it on a pixel-by-pixel basis using all data points. The simulation results demonstrate that both approaches provide high image quality, with the second approach having a slightly improved performance in the presence of noise.

10.18416/ijmpi.2023.2303082

II. Theory

In this work, we consider a 2D Lissajous trajectory as shown in Fig. 1a, where the DFs are applied along the x- and y-directions, and a two-channel acquisition is performed. According to the tensor-based theory of multichannel multidimensional x-space MPI, the multidimensional image tensor can be expressed in 2D as [3]:

$$\mathbf{\Omega}(\mathbf{x}) = \rho(\mathbf{x}) \ast\ast \mathbf{h}(\mathbf{x}) \tag{1}$$

$$= \begin{bmatrix} \hat{\rho}_{11}(\mathbf{x}) & \hat{\rho}_{12}(\mathbf{x}) \\ \hat{\rho}_{21}(\mathbf{x}) & \hat{\rho}_{22}(\mathbf{x}) \end{bmatrix}, \tag{2}$$

where

$$\mathbf{h}(\mathbf{x}) = \begin{bmatrix} h_{11}(\mathbf{x}) & h_{12}(\mathbf{x}) \\ h_{21}(\mathbf{x}) & h_{22}(\mathbf{x}) \end{bmatrix}. \tag{3}$$

Here, $\mathbf{\Omega}(\mathbf{x}) \in \mathbb{R}^{2x2}$ is the image tensor, $\mathbf{h}(\mathbf{x}) \in \mathbb{R}^{2x2}$ is the point spread function (PSF) tensor, $\rho(\mathbf{x})$ is the magnetic nanoparticle (MNP) distribution. and $\ast\ast$ denotes 2D convolution. The individual scalar images in the tensor can be expressed as $\hat{\rho}_{ij}(\mathbf{x}) = \rho(\mathbf{x}) \ast\ast h_{i,j}(\mathbf{x})$.

During a scanning trajectory, speed compensation of the acquired MPI signal yields a scalar image that can be expressed as [3]:

$$\hat{\rho}_{\mathbf{u}_a,\mathbf{u}_b}(\mathbf{x}) = \mathbf{u}_b^{\mathbf{T}} \mathbf{\Omega}(\mathbf{x}) \mathbf{u}_a(t) \,|_{\mathbf{x}=\mathbf{x}_s(t)}, \tag{4}$$

where $\mathbf{u}_a(t)$ is the unit trajectory vector at time t, $\mathbf{u}_b$ is the unit coil sensitivity vector, and $\mathbf{x}_s(t)$ is the instantaneous FFP position. Hence, the scalar MPI images acquired by receive coils placed along x- and y-directions can be expressed as:

$$\begin{bmatrix} \hat{\rho}_{\mathbf{u}_a,\mathbf{e}_1}(\mathbf{x}) \\ \hat{\rho}_{\mathbf{u}_a,\mathbf{e}_2}(\mathbf{x}) \end{bmatrix} = \mathbf{\Omega}(\mathbf{x}) \mathbf{u}_a(t) \,|_{\mathbf{x}=\mathbf{x}_s(t)}, \tag{5}$$

where $\mathbf{e}_1$ and $\mathbf{e}_2$ are the unit vectors along x- and y-directions, respectively.

Here, we propose computing the underlying scalar images $\hat{\rho}_{ij}(\mathbf{x})$ at the Lissajous node points (see Fig. 1a), where the trajectory passes through the same $\mathbf{x}$ position twice, but at different directions. Therefore, the resulting four scalar images can be represented as:

$$\begin{bmatrix} \hat{\rho}_{\mathbf{u}_{a_1},\mathbf{e}_1}(\mathbf{x}) & \hat{\rho}_{\mathbf{u}_{a_2},\mathbf{e}_1}(\mathbf{x}) \\ \hat{\rho}_{\mathbf{u}_{a_1},\mathbf{e}_2}(\mathbf{x}) & \hat{\rho}_{\mathbf{u}_{a_2},\mathbf{e}_2}(\mathbf{x}) \end{bmatrix} = \mathbf{\Omega}(\mathbf{x}) \mathbf{U}_a, \tag{6}$$

where we define $\mathbf{U}_a \in \mathbb{R}^{2x2}$ as the trajectory matrix whose columns are $\mathbf{u}_{a_1}$ and $\mathbf{u}_{a_2}$ which are the instantaneous trajectory vectors at the two time instances when the FFP passes through a node. Using Eq. 6, we can resolve the image tensor as:

$$\mathbf{\Omega}(\mathbf{x}) = \begin{bmatrix} \hat{\rho}_{\mathbf{u}_{a_1},\mathbf{e}_1}(\mathbf{x}) & \hat{\rho}_{\mathbf{u}_{a_2},\mathbf{e}_1}(\mathbf{x}) \\ \hat{\rho}_{\mathbf{u}_{a_1},\mathbf{e}_2}(\mathbf{x}) & \hat{\rho}_{\mathbf{u}_{a_2},\mathbf{e}_2}(\mathbf{x}) \end{bmatrix} \mathbf{U}_a{}^{-1}. \tag{7}$$

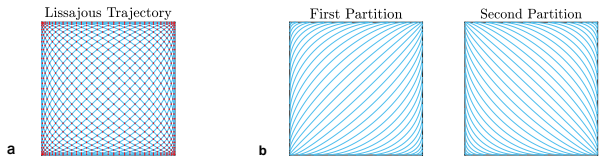

Figure 1: (a) 2D Lissajous trajectory and its nodes (marked in red). The trajectory passes through the nodes twice but at different directions. (b) Two partitions of the Lissajous trajectory with approximately 45° and 135° angles.

Hence, the four scalar images comprising the image tensor can be resolved, as long as the trajectory matrix is invertible. To satisfy this condition, the trajectory should pass through the nodes at two non-collinear directions. The Lissajous trajectory is well-suited for this problem, as it satisfy this requirement, and has nodes widely distributed across the field-of-view (FOV).

III. Methods and Materials

MPI simulations were performed using an in-house script in MATLAB, assuming an FFP scanner with selection field gradients of (3, 3, -6) T/m. For the Lissajous trajectory, the DF frequencies were set using the following relation [5]:

$$f_y = \frac{N_p}{N_p - 1} f_x, \tag{8}$$

where N_p is the trajectory density parameter, and f_x and f_y are the DF frequencies along x- and y-directions, respectively. Here, $f_x = 25$ kHz and $f_y = 25.36$ kHz were utilized, corresponding to $N_p = 70$. The DF amplitude was set to cover a 2×2 cm^2 FOV. A digital imaging phantom depicting a vasculature structure was utilized (see Fig. 2a). The MPI signal was sampled at 2.5 MHz sampling rate. Direct feedthrough interference and filtering were not incorporated in the simulations.

Two different variants of the proposed technique were implemented for image reconstruction. In the first variant, $\mathbf{\Omega}(\mathbf{x})$ was reconstructed at the Lissajous nodes only, as explained in Eq. 7. For this purpose, the speed-compensated signals from the two coils were interpolated to the node locations. Then, Eq. 7 was solved at the node points and scattered interpolation was utilized to interpolate the scalar images to a 2D grid.

While reconstruction at the nodes is practical for a dense Lissajous trajectory, it only utilizes the received signal at the nodes and disregards all other data points. Therefore, an alternative variant was implemented utilizing all data points. As shown in Fig. 1b, the Lissajous trajectory was partitioned into two segments according to the trajectory vector [5, 6]. Partitions consisted of data points with approximately 45° and 135° scanning angles, respectively. The speed-compensated signals from each

10.18416/ijmpi.2023.2303082

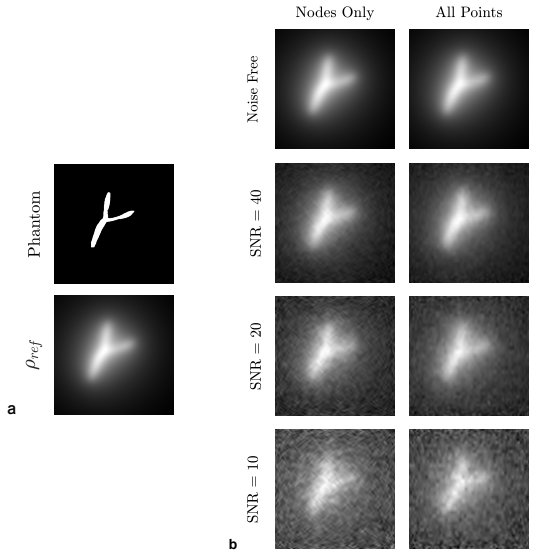

Figure 2: (a) Imaging phantom and the reference isotropic image, ρ_{ref} (b) Reconstructed ρ_{iso} images for nodes only and all points approaches, for the noise-free case and at different SNR levels between 10-40.

partition were interpolated onto a 2D grid using scattered interpolation to get two images per partition (i.e., one image per receive channel). Similarly, the trajectory angles of each partition was also interpolated to the same 2D grid. Then, for each pixel on the grid, Eq. 7 was solved, and $\mathbf{\Omega(x)}$ was reconstructed on a pixel-by-pixel basis.

Next, for each variant, $\rho_{\text{iso}} = \hat{\rho}_{11} + \hat{\rho}_{22}$ was formed to create a combined image with isotropic resolution. To compare the performance of the two methods, Monte Carlo simulations with 100 repetitions were conducted with signal-to-noise ratio (SNR) ranging between 5 to 100, together with the noise-free case. Here, SNR was defined as the ratio of the peak MPI signal and the standard deviation of the white Gaussian noise added. Note that $\hat{\rho}_{12}$ and $\hat{\rho}_{21}$ were also recovered but not utilized, as they had poor image quality and resolution due to the associated transverse PSFs [2].

Finally, the peak signal-to-noise ratio (PSNR) metric was utilized for quantitative evaluations:

$$PSNR = 10\log_{10}\left(\frac{\max^2(\rho_{\text{ref}})}{MSE}\right), \tag{9}$$

where ρ_{ref} is the reference combined image (see Fig. 2a), and MSE is the mean squared error between the reference combined image and the reconstructed ρ_{iso}. Here, ρ_{ref} was created by adding $\hat{\rho}_{11}$ and $\hat{\rho}_{22}$ of the original multidimensional image tensor from Eq. 2, which was computed using the associated PSF tensor in Eq. 3 (see [3] for details of the PSF tensor).

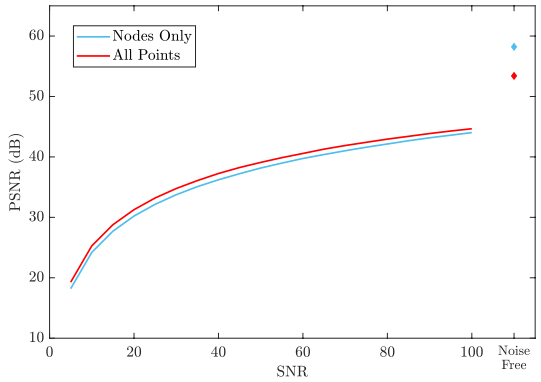

Figure 3: Performance comparison of the two variants at different SNR levels. The noise-free results are also marked.

IV. Results and Discussion

In Fig. 2b, reconstructed ρ_{iso} images are displayed for the two variants of the proposed method, for the noise-free case and for SNR = 40, 20, and 10. Both the variant that reconstructs the image using the node points only and the variant that reconstructs the images using all data points provide visually comparable image qualities.

Figure 3 shows the PSNR comparison of the two methods, plotting the average PSNR of 100 repetitions of Monte Carlo simulations, for SNR levels ranging between 5 to 100. The results of the noise-free case are also provided, displaying very high PSNR values exceeding 50 dB for both variants (i.e., near-ideal reconstructions). When noise is included, the variant using all points demonstrates slightly better performance than the one using the nodes only. When the proposed methods are evaluated at lower trajectory densities, both methods had lower performance than at higher densities, but their performances remained comparable (results not shown).

Note that both methods solve the same linear system of equations in Eq. 7, but at different number of points. Solving at the nodes only has a computational complexity of $O({N_p}^2)$, since the number of nodes is approximately proportional to the square of N_p. In contrast, solving at all grid points has a computational complexity of $O(N^2)$ for an $N \times N$ image. Since $N \gg N_p$ in general, the "nodes only" approach is computationally more efficient, with minimal loss of performance in the presence of noise.

Previously, a combined isotropic image was achieved by using two separate acquisitions with orthogonal 1D DFs [3, 4]. Another study proposed a gridding-based x-space reconstruction for non-Cartesian trajectories, but this approach was not able to resolve the true isotropic image [5]. Here, we extended the multidimensional tensor formalism to enable the reconstruction of the true isotropic MPI image for the Lissajous trajectory by taking advantage of its self-crossing property. This approach has the potential to be applied to other self-crossing tra-

10.18416/ijmpi.2023.2303082

jectories with multidimensional DFs, such as the radial Lissajous and bidirectional Cartesian trajectories [5].

Note that the effects of direct feedthrough filtering were not included in these simulations, as there is no ground-truth reference image for that case. Utilizing a direct feedthrough filter may cause a trajectory-dependent error when resolving the image tensor. Investigating such effects, developing methods to recover the filtered-out components, and experimentally verifying the proposed methods remain as important future work.

V. Conclusion

In this work, we presented an x-space reconstruction technique for resolving the multidimensional image tensor for the 2D Lissajous trajectory. The first variant of the proposed method takes advantage of the self-crossing property of the Lissajous trajectory, along with its nodes being widely distributed across the FOV. The second variant utilizes the fact that the Lissajous trajectory can be partitioned to allow reconstruction on a pixel-by-pixel basis. Both approaches provide successful reconstruction of the isotropic x-space MPI image.

Acknowledgments

This work was supported by the Scientific and Technological Research Council of Turkey (TUBITAK 120E208).

Author's statement

Conflict of interest: Authors state no conflict of interest.

References

[1] P. W. Goodwill and S. M. Conolly. The x-space formulation of the magnetic particle imaging process: 1-d signal, resolution, bandwidth, snr, sar, and magnetostimulation. *IEEE Transactions on Medical Imaging*, 29(11):1851–1859, 2010, doi:10.1109/TMI.2010.2052284.

[2] P. W. Goodwill and S. M. Conolly. Multidimensional x-space magnetic particle imaging. *IEEE Transactions on Medical Imaging*, 30(9):1581–1590, 2011, doi:10.1109/TMI.2011.2125982.

[3] K. Lu, P. Goodwill, B. Zheng, and S. Conolly. Multi-channel acquisition for isotropic resolution in magnetic particle imaging. *IEEE Transactions on Medical Imaging*, 37(9):1989–1998, 2018, doi:10.1109/tmi.2017.2787500.

[4] F. Werner, N. Gdaniec, and T. Knopp. Improving the spatial resolution of bidirectional cartesian mpi data using fourier techniques. *International Journal on Magnetic Particle Imaging*, 3(1), 2017.

[5] A. A. Ozaslan, A. Alacaoglu, O. B. Demirel, T. Çukur, and E. U. Saritas. Fully automated gridding reconstruction for non-cartesian x-space magnetic particle imaging. *Physics in Medicine & Biology*, 64(16):165018, 2019, doi:10.1088/1361-6560/ab3525.

[6] O. A. A. Alacaoglu A and S. E. U. Nonlinear scanning in x-space mpi. *Int. Workshop on Magnetic Particle Imaging (Book of Abstracts)*, (74), 2016.

